PCCP

COMMUNICATION

View Article Online
View Journal

Cite this: DOI: 10.1039/d5cp03827h

Received 3rd October 2025,
Accepted 17th November 2025

DOI: 10.1039/d5cp03827h

rsc.li/pccp

Sweet optimization: glucose-vitrified samples for hyperpolarizing glutamine in biological studies

Léa Gutierrez, †[a] Karen Dos Santos, †[bc] Mehdi Soussi-Therond, [ad] Aiky Razanahoera, [d] Daniel Abergel, [d] Nicolas Giraud *[a] and Mathieu Baudin *[ad]

This work describes the development of a versatile formulation using glucose as a vitrification agent in dynamic nuclear polarization. Significantly high polarization levels are achieved through optimization of a sample formulation, using sodium acetate and glutamine as targets. The best optimized formulation allowed precise monitoring of the enzymatic conversion of glutamine to glutamate, paving the way for advances in cellular metabolism applications.

1. Introduction

NMR enhanced by dissolution-dynamic nuclear polarization (dDNP) has, among numerous applications,[1,2] facilitated the exploration of cellular metabolism.[3] It holds significant value in discerning the metabolic by-products of amino acids, which can serve as biomarkers for various diseases. However, the widespread use of dDNP is limited by the availability of suitable metabolic tracers. Indeed, hyperpolarizing a new metabolite to acquire highly sensitive magnetic resonance (MR) data when it is involved in a complex biological system requires optimizing an adapted formulation of this molecule. This is for instance the case for glutamine, which has been shown to play a key role in a broad number of biological processes.[4] In a previous study, we have highlighted the role of glutamine as a bio-probe after its conversion into glutamate by glutaminase.[5] It is involved in the reactive oxygen species regulation,[6] in GABA metabolism for modulation of the central nervous system and once converted to α-ketoglutarate, it enters the tricarboxylic acid cycle for cellular energy supply.[7]

State-of-the-art dDNP sample formulations consist of a free radical compound and a solvent mixture that includes water, usually deuterated and non-deuterated. Moreover, a vitrification or so-called "glassing" agent, such as glycerol-d_8, is added to ensure a homogenous distribution of radicals. The choice of this glassing agent is essential for achieving a uniform distribution of the radicals across the sample. In dDNP, particular attention is paid to cryoprotection to avoid phase separation during freezing of the sample and the formation of microcrystals. Glycerol has emerged as the preferred solution for *in vivo* studies based on its favourable safety profile for the user and relatively high glassing efficiency.[8] While it is safe at concentrations used in DNP studies, it is not chemically inert,[9,10] and one may want to avoid its use for studies under near-physiological conditions to obtain relevant data from biological samples. Additionally, spectral overlaps between the carbon-(^{13}C) signals of glycerol[11] and our products of interest can potentially impede the extraction of kinetic constants.

Pioneering works such as those by Karlsson *et al.* in 2012[12] or Miclet *et al.* in 2014[13] have already used glucose as a glassing agent. But so far, none have involved systematic optimization of its concentration and its impact on the achieved polarization, as it was the targeted analyte to polarize. Recent studies have also extensively explored the use of alternative sugars or salts, such as trehalose[8] and NaCl,[14] which have shown promising glassing properties in DNP sample formulations. Building on this line of research, we focus here on glucose as a biologically interesting alternative to common glassing agents. It is a non-expensive compound, naturally present in cells, like glutamine, and can also serve as an additional molecular probe.[15,16] This monosaccharide is commonly used as a pharmaceutical excipient to protect, feed and bring energy to cells in formulations of biological drugs.[17] Finally, it is often chosen due to its biocompatibility with a wide range of medications and its innocuity. Glucose has an exceptionally high glass transition temperature,[18] due to its

[a] *Laboratoire de Chimie et Biochimie Pharmacologiques et Toxicologiques, Université Paris Cité, 45 rue des Saints Pères, 75006 Paris, France. E-mail: nicolas.giraud@u-paris.fr, mathieu.baudin@u-paris.fr*
[b] *Athinoula A. Martinos Center for Biomedical Imaging, Massachusetts General Hospital, Harvard Medical School, 149 13th St., Charlestown, MA, USA*
[c] *Polarize ApS., Asmussens Alle 1, 1808 Frederiksberg, Denmark*
[d] *Chimie Physique et Chimie du Vivant (CPCV), Département de Chimie, École Normale Supérieure, PSL University, Sorbonne Université, CNRS, 75005 Paris, France*
† L. Gutierrez and K. Dos Santos contributed equally to this work as the first authors.

anisotropic hydrogen bonding pattern, which prevents ice nucleation and promotes the formation of amorphous glasses over ordered crystalline solids or liquids.

In this work, we explore the use of glucose as an interesting alternative to common glassing agents. To do so, we optimize its concentration in dDNP samples for two substrates with respect to the polarization value, and test the obtained formulation on an application, *i.e.*, the enzymatic conversion of glutamine to glutamate by the glutaminase enzyme.

2. Experimental

2.1. Materials

2.1.1. Solid state experiments. The preparation of the solution was straightforward using a precision balance and standard laboratory pipettes since the sample we obtained was not as viscous as glycerol. 3 M of [1-^{13}C]sodium acetate was dissolved in 40 mM of TEMPOL (4-hydroxy-2,2,6,6-tetramethylpiperidine-1-oxyl), 90% of D_2O, 10% of H_2O to yield 100 μL of solution as the paramagnetic polarizing agent. This formulation was followed by the addition of different amounts of non-labelled D-glucose with concentrations ranging from 0.25 M to 5 M depending on the sample in order to promote glass formation. Beads of 20 μL of these solutions were then frozen in a liquid nitrogen Dewar and introduced into a 6.7-T polarizer operated at a temperature of 1.2 K. For each sample, both ^{1}H and ^{13}C NMR experiments were conducted, including ^{1}H and ^{13}C thermal equilibrium buildup measurements at 4.2 K, as well as ^{1}H and ^{13}C DNP buildups using two different cross-polarization (CP) sequences:[19–21]

– The first used a 10-ms spin-lock between two adiabatic half-passages applied on both channels (WURST, 200 kHz, 600 ms). Respective powers applied during the spin-lock pulses were 80 W on ^{13}C and 10 W on ^{1}H respectively, with a 100–50–100 ramp on ^{13}C.

– The second used a pair of adiabatic inversion pulses on both channels (WURST, 200 kHz, 12 ms, 50 W on ^{13}C and 8 W on ^{1}H).

Depending on the sample, three to five CP contacts were required to achieve a maximal ^{13}C polarization value, with a delay of 4 minutes between each one. Depending on the sample, the CP sequences performed slightly differently, with an error of about 10% between them. The result reported in Fig. 1B was the best achieved polarization between the two sequences for each sample.

A series of 1D spectra were acquired to generate polarization buildup curves. Small flip angle pulses (1° and 5° for ^{1}H and ^{13}C respectively) were used to avoid perturbing the polarization accumulation. Microwave irradiation was performed using an Elva-1 source coupled with a frequency doubler delivering microwaves at 187.94 GHz and a power of 120 mW before the doubler. Microwave gating was used to enhance the efficiency of CP transfers until a stationary ^{13}C polarization was reached.[22] The measurement of the ^{1}H background signal was performed for each series of experiments (Fig. S1) and was subtracted from the measured signal to calculate polarization values (eqn (S1) and (S2)). No measurable ^{13}C background was observed.

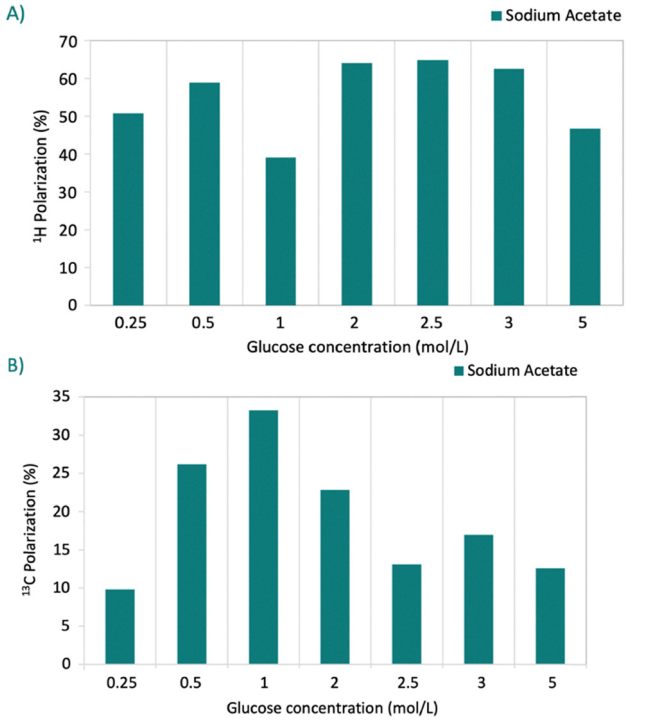

Fig. 1 Polarization values for (A) ^{1}H and (B) ^{13}C nuclei obtained for 3 M [1-^{13}C]sodium acetate. Experiments were performed using a 6.7 T polarizer at 1.2 K, with glucose concentrations ranging from 0.25 to 5 M.

300 mM of [5-^{13}C] glutamine was dissolved in 40 mM TEMPOL, 90% D_2O, and 10% H_2O, followed by the addition of natural abundance D-glucose at concentrations ranging from 1 M to 5 M depending on the sample.

2.1.2. Liquid state experiments. The most efficient formulation of [5-^{13}C] glutamine was dissolved in a solution of 5 mL D_2O. Small flip-angle pulses of 10° were applied for detection every second while the substrate returned to thermal equilibrium polarization.

The same formulation of [5-^{13}C] glutamine sample was dissolved in a 40-mM sodium acetate buffer pH 5.0 containing H_2O/D_2O (90/10) and 100 U of glutaminase activity (determined according to the supplier – NZYtech 2500 U in 1 mL suspension).

2.2. Methods: kinetic model

The evolutions of hyperpolarized signals on the resulting ^{13}C spectra (Fig. 5) were modelled using simple first-order kinetic equations incorporating the enzymatic reaction that converts the substrate S to the product P with a conversion rate k as well as longitudinal relaxation times of glutamine and glutamate.

The mathematical model is described using eqn (1) and (2):

$$\frac{dS}{dt} = -k \times S(t) - \frac{1}{T_{1s}} \times S(t) \quad (1)$$

$$\frac{dP}{dt} = k \times S(t) - \frac{1}{T_{1p}} \times P(t) \quad (2)$$

where S denotes the [5-^{13}C] glutamine magnetization and T_{1s} its longitudinal relaxation time. P is the [5-^{13}C] glutamate magnetization

and T_{1p} is its longitudinal relaxation time. The datasets containing the signals from the substrate and the product were first normalized using the maximum signal of the glutamine, allowing for a direct comparison between them. Data processing and analysis, including mathematical fitting and the determination of kinetic constants, were performed using a custom-written Python program.

3. Results and discussion

To do so, we first performed a preliminary round of experiments to optimize the polarization of sodium acetate samples. This well-known metabolite, which is commonly used in dDNP due to its abundance in the biological media, low cost and ease of polarization,[23] was chosen here as a model to explore several experimental conditions. Fig. 1 presents the ^{1}H and ^{13}C polarization values obtained in this feasibility study as a function of glucose concentration for samples containing 3 M [1-^{13}C]sodium acetate.

As shown in Fig. 1A, a ^{1}H polarization maximum of approximately 65% is reached for glucose concentrations between 2 and 3 M. However, it is important to note that for glucose concentrations exceeding 2.5 M, the acetate polarization decreased, and for these samples, the polarization buildup was too slow to be used efficiently for CP in practice (Fig. S2). In fact, ^{1}H buildup dynamics were fastest for 1 M glucose (Fig. S3), which likely explains the optimum found in ^{13}C polarization measurements described below. We also observed that the polarization buildup times were similar to the ones obtained with the conventional sample formulation using glycerol, also known as "DNP juice". In principle, a larger proton polarization should entail a larger cross-polarization transfer to ^{13}C. However, we did not observe a similar behaviour between ^{1}H and ^{13}C polarization. Instead, an optimal glucose concentration of 1 M was observed, yielding a solid-state polarization of $P(^{13}C)$ = 33%. This value is comparable to the polarization level achieved using a standard glycerol-d_8 formulation,[5] thereby demonstrating that the sample formulation with glucose is effective for sodium acetate. Furthermore, we optimized the protonation level of the DNP juice by adjusting the H_2O content of the sample. The results shown in Fig. S4 confirm that a suitable condition is obtained with 10% H_2O in the sample. We then proceeded to determine the glucose concentration in the "DNP juice" for optimal glutamine polarization.

Fig. 2 illustrates the solid-state ^{1}H polarization obtained for glutamine as a function of glucose concentration in the sample following the protocol used for sodium acetate.

We observe that ^{1}H polarization increases with the concentration of the glassing agent, with a maximum polarization close to 70% achieved at a glucose concentration of 4 M. From 3 M glucose onwards, the sample exhibited the transparency typically associated with amorphous freezing, which is known to yield improved polarization. Examples of the appearance of the frozen beads are shown in Fig. 3. At glucose concentrations above 5 M, the sample solubility significantly decreased and required prolonged sonication and strong heating; therefore no further measurements were conducted.

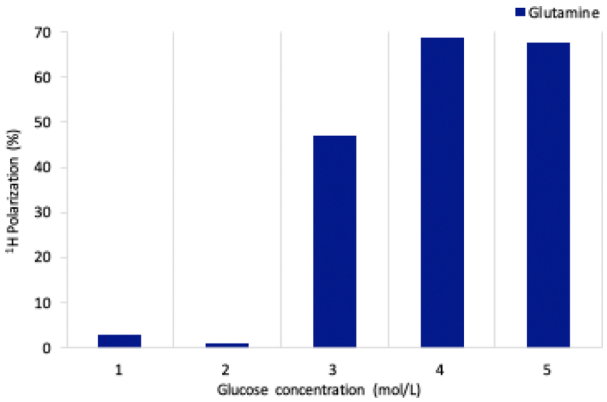

Fig. 2 ^{1}H polarization values obtained with [5-^{13}C] glutamine at 300 mM concentration. Experiments were performed using a 6.7 T polarizer at 1.2 K, with glucose concentrations ranging from 1 to 5 M.

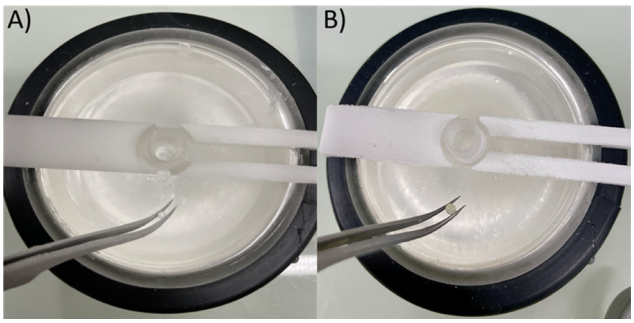

Fig. 3 [5-^{13}C] glutamine sample in beads formed using glucose as a glassing agent: (A) 20 μL bead with 1 M glucose; (B) 20 μL bead with 4 M glucose.

Following this sample optimization, the hyperpolarized glutamine samples were dissolved to provide a blank sample. Strong ^{13}C signals were detected in the liquid state, as shown in Fig. 4.

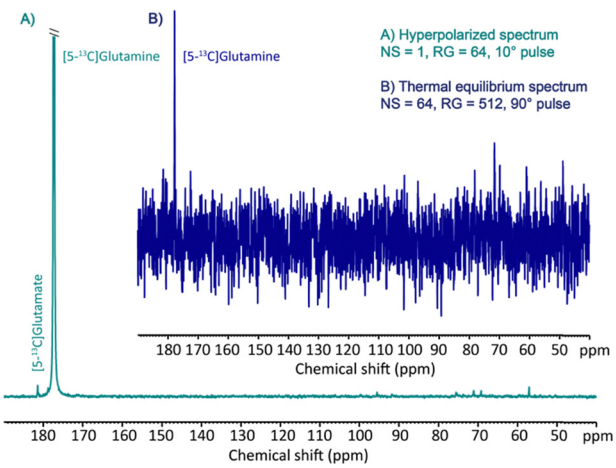

Fig. 4 (A) Hyperpolarized ^{13}C spectrum of a 300 mM [5-^{13}C] glutamine sample recorded after dissolution and transfer in a 400-MHz spectrometer (in green), from a single dDNP scan using a 10° flip-angle (NS = 1, RG = 64). (B) Thermal spectrum acquired in 5 h (in blue) at 298 K with a 90° pulse (NS = 64, RG = 512).

The dDNP spectrum in Fig. 4A exhibits the enhanced ^{13}C signals of [5-^{13}C]glutamine and [5-^{13}C] glutamate in the 176–183 ppm region,[5] illustrating a significantly increased ^{13}C sensitivity. The [5-^{13}C] glutamate signal at 180.4 ppm is due to residual [5-^{13}C] glutamate from the [5-^{13}C]glutamine sample supplier. The ^{13}C signal enhancement in the liquid state was calculated by the comparison of a single peak intensity in the thermal equilibrium spectrum recorded in 5 h (Fig. 4B) with the hyperpolarized signal obtained from the same sample in a single scan (Fig. 4A). We estimated a 24% polarization in a glutamine sample using glucose as the glassing agent. It is noteworthy that the glucose is detectable between 55 and 100 ppm despite being present at a natural abundance in the sample. The ^{13}C signal decay of a sample of [5-^{13}C] glutamine was still observed after two minutes (Fig. S5), providing a suitable time window to monitor the *in vitro* conversion of glutamine to glutamate through the action of glutaminase.

Next, the hyperpolarized glutamine samples were dissolved in a buffer solution containing glutaminase. A representative example of these experiments is illustrated in Fig. 5.

The decay of the glutamine, and the buildup and decay of the glutamate signals, were observed, attesting for the successful enzymatic conversions of glutamine to glutamate by glutaminase. The observed decrease in glutamine (GLN) signal intensity results from both its conversion to glutamate (GLU) and longitudinal relaxation (T_{1s}), whereas the decrease of the glutamate signal is caused by its relaxation (T_{1p}) only.

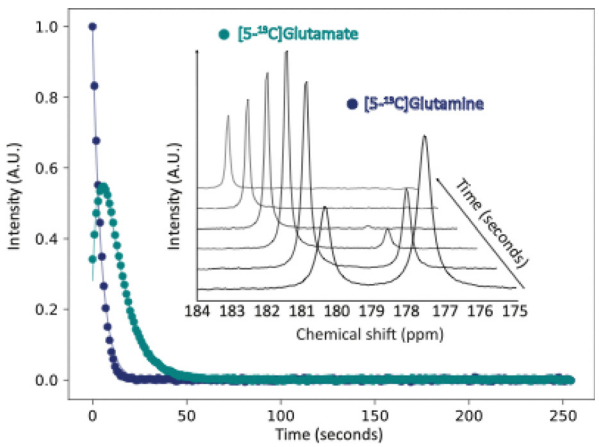

Fig. 5 Time evolution of hyperpolarized ^{13}C signals for [5-^{13}C] glutamine (177.6 ppm) and [5-^{13}C]glutamate (180.4 ppm). The plot shows the fit of a kinetic model to the experimental relative integrals of both metabolites over time, following dissolution in a 40-mM sodium acetate buffer pH 5.0 containing H_2O/D_2O (90/10) and 100 U of glutaminase.

The model fitted to the data using eqn (1) and (2) produced correlation coefficients R_2 of 0.995 and 0.997 for the triplicate experiment. The fast decay of the glutamine signal forced us to subsample our time points, leading to increased uncertainty in our fitted data especially in the early stages of the experiment as shown in the analysis of the residuals associated with the fit in SI (Fig. S6 and S7). To overcome this limitation, we constrained our model by fixing the T_1 value of glutamine to a literature-reported value[24,25] obtained under experimental conditions comparable to ours. Table 1 presents a comparison between kinetic constants extracted from a triplicate set of dDNP experiments using an unconstrained model and those obtained using a model in which the T_1 of glutamine was fixed at 22.3 seconds.

The average T_1 of glutamine was found to be T_{1s} = 23.3 ± 3.1 s after fitting without constraint. The production of glutamate was monitored in this time course experiment, and its relaxation time was found, on average as well, to be T_{1p} = 9.9 ± 1.1 s. Despite the uncertainty in the initial data points, both fitting methods yielded consistent and accurate results in agreement with literature values, confirming the reliability of the extracted parameters. The apparent conversion rates k_{obs} were also comparable using these two fitting approaches, which allowed us to subsequently calculate normalized conversion rates k_{norm}, providing a more relevant measure of the process. The k_{norm} value of glutamine to glutamate was calculated to be 6.40 × 10^{-3} mM per L.s.U based on the apparent k_{obs} value adjusted from the fit, and normalized using the enzyme activity (100 U) and the injected substrate concentration, which was quantified at thermal equilibrium after the dissolution experiments. This value is sufficiently close, with only reasonable experimental variability, and remains within the same order of magnitude as our previous results (Table S1), supporting the overall consistency of the method. The fact that a simple kinetic model is able to account for the kinetics has been noted previously,[16] and suggests that the dDNP measurements, in the case of a large enzymatic activity, actually starts when the substrate has already significantly decreased. The putative Michaelis kinetics is thus sufficiently well approximated using first order kinetics. More details about the data fitting and its challenges are presented in the SI. Overall, the quality of the obtained data demonstrates that high polarization levels can be consistently achieved using glucose as the glassing agent with good repeatability, paving the way to a

Table 1 Comparison of the values of the kinetic parameters extracted from our unconstrained model with those obtained by fixing the T_1 of [5-^{13}C]glutamine

	T_1 [5-^{13}C]GLN (s)			T_1 [5-^{13}C]GLU (s)			k_{obs} (s^{-1})		
Fitted values without constraint	26.7 ± 1.6	22.4 ± 1.1	20.8 ± 1.1	9.0 ± 0.1	11.1 ± 0.2	9.6 ± 0.1	0.1 ± 1.9 × 10^{-3}	0.1 ± 1.9 × 10^{-3}	0.2 ± 2.1 × 10^{-3}
Average values	23.3 ± 3.2			9.9 ± 1.0			0.1 ± 3.2 × 10^{-2}		
Fitted values with a fixed T_1 GLN	22 ± 3.3			9.4 ± 5.6 × 10^{-2}	11.0 ± 8.4 × 10^{-2}	9.5 ± 5.3 × 10-02	0.1 ± 9.1 × 10^{-4}	0.1 ± 1.1 × 10^{-3}	0.2 ± 1.4 × 10^{-3}
Average values, fixed T_1 GLN	22 ± 3.3			10.0 ± 0.9			0.1 ± 3.2 × 10^{-2}		

reliable determination of kinetic parameters for reaction processes such as the model one discussed here.

Conclusions

Throughout this investigation, an optimized sample formulation using glucose as the glassing agent was established both for acetate and glutamine for enhanced polarization performances and real-time enzymatic analysis. We demonstrated the possibility of replacing glycerol by glucose to produce hyperpolarized ^{1}H and ^{13}C spectra of various analytes in a single experiment. The glassing effect of glucose ensures sample homogeneity and uniform radical distribution, supporting its viability for dDNP experiments. Though still in its early stage, this new sample formulation opens new avenues for polarizing biological samples with increased performance and can be easily implemented for other metabolites. Kinetic and relaxation values obtained align closely with previous studies. Further optimizations are anticipated, such as increasing the radical concentration for this formulation to easily accelerate the polarization buildup to its stationary polarization value. Besides, the study of a phase diagram to promote the amorphous form of glucose rather than its crystalline form is envisaged, as well as the solubility and maturation properties of the samples.[26] The objective here was to further explore sample optimization performance and align it with our biological application. One perspective of this study is the detection of low concentrations of ^{13}C-labeled or even natural abundance metabolites involved in glutamine metabolism in the liquid state, using glucose as a glassing agent. This approach holds potential for future co-polarization of both glutamine and glucose. While the addition of glucose will interfere with the metabolism, this effect will be leveraged to enable the simultaneous analysis of the kinetics of both substrates under physiological conditions—an aspect that will be further investigated within the research team. Therefore, these findings open new avenues using glucose as a glassing agent and co-analyte with glutamine to monitor simultaneously their metabolisms in biologically relevant systems, such as cancer cell media.

Author contributions

K. D. S., L. G. and D. A. performed conceptualization; L. G., M. B. and N. G. performed development of methodology and writing, review and revision of the paper; L. G., K. D. S., M. S.-T., A. R. provided acquisition, analysis and interpretation of data; M. B. provided technical and material support; M. B., N. G. supervised the research. All authors read and approved the final paper.

Conflicts of interest

The authors confirm that there are no conflicts of interest to declare.

Data availability

Data for this article including original datasets and fitting code is available in the supplementary information (SI) and at the following URL: **https://sdrive.cnrs.fr/s/mKa9Ccobk6Zeiqy**. Supplementary information is available. See DOI: **https://doi.org/10.1039/d5cp03827h**.

Acknowledgements

This work was funded by the French National Research Agency (grant ANR-22-CE29_0003-01 PolarGlu).

Notes and references

1 J. H. Ardenkjaer-Larsen, *eMagRes*, John Wiley & Sons, Ltd, 2018, pp. 63–78.
2 D. Kurzbach, E. Canet, A. G. Flamm, A. Jhajharia, E. M. M. Weber, R. Konrat and G. Bodenhausen, *Angew. Chem., Int. Ed.*, 2017, **56**, 389–392.
3 L. Salamanca-Cardona, H. Shah, A. J. Poot, F. M. Correa, V. Di Gialleonardo, H. Lui, V. Z. Miloushev, K. L. Granlund, S. S. Tee, J. R. Cross, C. B. Thompson and K. R. Keshari, *Cell Metab.*, 2017, **26**, 830–841.e3.
4 R. J. DeBerardinis and T. Cheng, *Oncogene*, 2010, **29**, 313–324.
5 K. Dos Santos, G. Bertho, C. Caradeuc, V. Baud, A. Montagne, D. Abergel, N. Giraud and M. Baudin, *Chem. Phys. Chem.*, 2023, **24**, e202300151.
6 C. T. Hensley, A. T. Wasti and R. J. DeBerardinis, *J. Clin. Invest.*, 2013, **123**, 3678–3684.
7 L. M. Phan, S.-C. J. Yeung and M.-H. Lee, *Cancer Biol. Med.*, 2014, **11**, 1–19.
8 J. R. Brender, S. Kishimoto, G. R. Eaton, S. S. Eaton, Y. Saida, J. Mitchell and M. C. Krishna, *Magn. Reson. Med.*, 2021, **85**, 42–48.
9 R. C. Tao, R. E. Kelley, N. N. Yoshimura and F. Benjamin, *J. Parenter. Enteral Nutr.*, 1983, **7**, 479–488.
10 T. Hibuse, N. Maeda, A. Nagasawa and T. Funahashi, *Biochim. Biophys. Acta, Biomembr.*, 2006, **1758**, 1004–1011.
11 J. Lu, P. Wang, Q. Wang, Y. Wang and M. Jiang, *Molecules*, 2018, **23**, 1177.
12 M. Karlsson, P. R. Jensen, J. Ø. Duus, S. Meier and M. H. Lerche, *Appl. Magn. Reson.*, 2012, **43**, 223–236.
13 E. Miclet, D. Abergel, A. Bornet, J. Milani, S. Jannin and G. Bodenhausen, *J. Phys. Chem. Lett.*, 2014, **5**, 3290–3295.
14 F. Ferrer, M. Juramy, R. Jabbour, S. Cousin, F. Ziarelli, G. Mollica, P. Thureau and S. Viel, *J. Phys. Chem. Lett.*, 2023, **14**, 9619–9623.
15 A. Sadet, E. M. M. Weber, A. Jhajharia, D. Kurzbach, G. Bodenhausen, E. Miclet and D. Abergel, *Chemistry*, 2018, **24**, 5456–5461.
16 M. Soussi-Therond, D. Guarin, A. Razanahoera, Y. Zhang, M. Baudin, E. Miclet, N. Giraud and D. Abergel, *J. Am. Chem. Soc.*, 2024, **146**, 34651–34660.
17 S. S. Bharate, S. B. Bharate and A. N. Bajaj, *J. Excipients Food Chem.*, 2010, **1**(3), 3–26.

18 A. Simperler, A. Kornherr, R. Chopra, P. A. Bonnet, W. Jones, W. D. S. Motherwell and G. Zifferer, *J. Phys. Chem. B*, 2006, **110**, 19678–19684.
19 A. J. P. Linde, PhD thesis, 2010, University of Notthingham, Nottingham.
20 S. J. Eliott, Q. Stern, M. Ceillier, T. El Daraï, S. F. Cousin, O. Cala and S. Janin, *Prog. Nucl. Magn. Reson. Spectrosc.*, 2021, **126–127**, 59–100.
21 S. J. Elliott, M. Ceillier, O. Cala, Q. Stern, S. F. Cousin and S. Jannin, *J. Magn. Reson. Open*, 2022, **10–11**, 100033.
22 A. Bornet, A. Pinon, A. Jhajharia, M. Baudin, X. Ji, L. Emsley, G. Bodenhausen, J. H. Ardenkjaer-Larsen and S. Jannin, *Phys. Chem. Chem. Phys.*, 2016, **18**, 30530–30535.
23 A. Flori, M. Liserani, F. Frijia, G. Giovannetti, V. Lionetti, V. Casieri, V. Positano, G. D. Aquaro, F. A. Recchia, M. F. Santarelli, L. Landini, J. H. Ardenkjaer-Larsen and L. Menichetti, *Contrast Media Mol. Imaging*, 2015, **10**, 194–202.
24 C. Cabella, M. Karlsson, C. Canapè, G. Catanzaro, S. Colombo Serra, L. Miragoli, L. Poggi, F. Uggeri, L. Venturi, P. R. Jensen, M. H. Lerche and F. Tedoldi, *J. Magn. Reson.*, 2013, **232**, 45–52.
25 F. A. Gallagher, M. I. Kettunen, S. E. Day, M. Lerche and K. M. Brindle, *Magn. Reson. Med.*, 2008, **60**, 253–257.
26 E. Weber, G. Sicoli, H. Vezin, G. Frebourg, D. Abergel, G. Bodenhausen and D. Kurzbach, *Angew. Chem., Int. Ed.*, 2018, **57**, 5171–5175.

